Research on Engineering Structures & Materials
www.jresm.org
Research Group

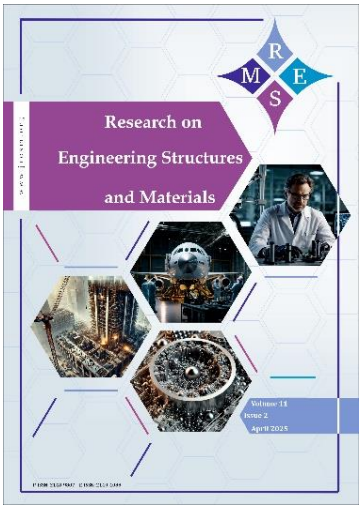

Strengthening of corroded reinforced concrete beam via optimized fiber reinforced self-compacting concrete jacket

Nada A. Mahmoud, Mahmoud Khashaa Mohammed, Yousif A. Mansoor

Online Publication Date: 20 December 2025

URL: http://www.jresm.org/archive/resm2026-1294ic1024rs.html
DOI: http://dx.doi.org/10.17515/resm2026-1294ic1024rs

Journal Abbreviation: *Res. Eng. Struct. Mater.*

To cite this article
Mahmoud N A, Mohammed M K, Mansoor Y A. Strengthening of corroded reinforced concrete beam via optimized fiber reinforced self-compacting concrete jacket. *Res. Eng. Struct. Mater.*, 2026; 12(2): 1087-1100

Research on Engineering Structures & Materials
www.jresm.org
Research Group

Research Article

Strengthening of corroded reinforced concrete beam via optimized fiber reinforced self-compacting concrete jacket

Nada A. Mahmoud [*,a], Mahmoud Khashaa Mohammed [b], Yousif A. Mansoor [c]

Civil Engineering Department, University of Anbar, Ramadi, Iraq

Article Info

Article History:

Received 24 Oct 2025

Accepted 19 Dec 2025

Keywords:

Micro steel fibers;
Self-compacting Concrete;
Optimization;
Strength;
Strengthening

Abstract

In this paper, an experimental study is presented on a wide variety of fresh and hardened characteristics of an optimized steel fiber-reinforced self-compacting concrete (SFRSCC) mix. This is in order to examine the possibility of using this type of concrete to strengthen a corroded RC concrete beam with dimensions of 150×200×1200 mm. Micro steel fibers MSF were utilized at percentages of 0, 0.25, 0.5, 0.75, and 1% by volume. Using multi-objective optimization approach SFRSCC mix is optimized based on multi responses (tested properties). The theoretical optimization and its verification based on testing different fresh properties (slump flow, T500, L-box and segregation resistance), mechanical properties (compressive, flexural, splitting tensile strength, and modulus of elasticity), in addition to related durability properties (porosity and water absorption). In this investigation, the results of the experiments indicated that steel fibers enhanced the compressive, flexural, tensile strength, and elastic modulus as well as sieve segregation test by 22.9, 77.9, 112.8, 18.3, and 55.6% respectively which was achieved using 1% percentage of steel fiber. However, the rest of the properties are negatively affected due to the rise in fiber content. Thus, it was decided to implement a multi objective optimization process to get the optimum content. The optimum SCC mixture that satisfies all requirements was found using statistical software (Minitab 2018). The theoretical chosen optimal ratio of 0.47% of fibers that was obtained through optimization and it was evaluated and empirically verified. The optimal ratio was used in SCC mix for strengthening purposes with 30 mm jacket thickness for corroded RC beam. Strengthen corroded RC beam showed a considerable increase in its bending capacity, around 20%, contrasted to the corroded beam. The utilization of this method of strengthening also increased the ultimate load at first crack and the stiffness. Thus, it can be deduced that the method used is an effective method of strengthening.

1. Introduction

Self-compacting concrete SCC is a very flowing and non-segregating concrete composition. There is no need for vibration to condense which results in less noise and significant labor effort savings as well as lower cost which improves the economics of concrete production [1]. Similar to normal vibrated concrete (NVC), SCC mixes include aggregate, cement, water, admixtures, and specific mineral additions or fillers. To improve its flowing characteristics, SCC has a higher dosage of superplasticizers and fillers (such as fly ash, silica fume, limestone powder, etc.) than NVC [2]. In SCC, there is a high possibility to use replacement materials instead of cement to maintain the same compressive strength while reducing the amount of cement. Thus, it may be classified as a sustainable material [3, 4]. Self-compacting concrete requires more paste than conventional concrete for high flowability, requiring 500-600 kg/m^3 of powder material. Portland cement, used in SCC mixes, emits CO2 into the atmosphere, negatively impacting the environment. High cement

*Corresponding author: nad21e1006@uoanbar.edu.iq
[a]orcid.org/ 0009-0005-6412-869X; [b]orcid.org/ 0000-0003-4817-8396; [c]orcid.org/0000-0002-5235-7904
DOI: http://dx.doi.org/10.17515/resm2026-1294ic1024rs

content also produces hydration heat, leading to concrete cracking during the hydration process. Therefore, SCC mixes require more powder material for self-compacting capability [5].

Fly ash is a byproduct of pulverized coal burning, which can be used in producing high strength self-compacting concrete (SCC) due to its pozzolanic properties. This well-grained dust, primarily composed of Al_2O_3 and SiO_2, can improve particle size distribution, increase concrete strength, and create a compacted microstructure. It also facilitates easier displacement of aggregate grains, making it a crucial component of self-compacting concrete mixtures. Therefore, fly ash's potential in SCC production is significant [6]. Guo et al. [7] found that silica fume (SF) addition improves SCC performance and is a popular replacement for concrete produced by silicon and ferrosilicon industries. SF increases concrete's toughness, compressive, tensile, and flexural strengths and influences elastic modulus. It also makes concrete resistant to chemical attacks, making it suitable for marine constructions, highway bridges, and parking decks. Steel fibers are added to SCC to improve mechanical properties, including post-cracking load bearing and energy absorption performance. They reduce crack size, enhancing concrete strength. However, increased crack width increases concrete permeability, promoting steel reinforcement corrosion. Fiber reinforcing techniques enhance concrete's ductility and post-cracking resistance [8].

Fibers significantly influence the workability of freshly poured concrete, with the type, amount, and matrix affecting the material's workability. A good fiber distribution is crucial for optimal benefits. The better performance of hardened concrete must be balanced with the appropriate workability of fresh concrete. The number of fibers added depends on the fiber type and mixture composition [9]. Abid [10] investigated the behavior of Micro-steel fiber-reinforced SCCs to flexural impact. Eight mixtures with two design grades of 30 and 50 MPa have been produced in order to differentiate between regular and high-strength SCCs. The fiber content, which came in four volumetric values of 0, 0.5, 0.75, and 1.0%, served as the differentiating factor for each design grade. The study discovered that adding micro-steel fibers significantly improved impact resistance and ductility, with higher percentage improvements in the failure stage contrasted to the cracking stage. The largest gains for combinations of 30 MPa were 543% and 836%.

The most common deteriorating process for structural elements made of reinforced concrete is corrosion of the steel reinforcement. Steel tends to return to its initial state (ore) by an electrochemical process that produces iron oxides on the coating (rust) [11]. Fayaad [12] showed that the ultimate load has been severely affected by the percentage of corrosion mass loss. In comparison to a reference concrete beam that was not corroded, the failure load decreased by about 14 and 27 percent, for each, as the percentage of corrosion mass loss increased by 8.25 and 14.15%. A common area of concrete researches' nowadays is strengthening preexisting RC beams which can effectively increase their service lives. Abdul Hameed [13] investigated damaged concrete beam repair using fiber-reinforced self-compacting concrete (FR-SCC). According to the study, better FR-SCC mixtures are effective at increasing the cracking stress on repaired beams, which can prolong their life. The study also considered using polypropylene fiber PPF in SCC. However, this study considered the use of polypropylene fiber PPF in SCC and it took only the fresh properties to optimize their volume fraction before used it for strengthening purpose.

However, few research work has been found in the literature addressing the use of optimized SCC for strengthening of corroded reinforced concrete beams. Therefore, the current study looks into how to reinforce a corroded RC beam using an optimal steel fibers SCC mix. A multi-objective optimization approach was used, considering different volume fractions of steel fibers in SCC and their responses in both fresh and hardened properties. The tested properties included flowability, T500, pasting ability, and segregation resistance, while the hardened properties included compressive strength, splitting tensile strength, flexural strength, modulus of elasticity, porosity, and absorption. The theoretical optimized volume fraction was experimentally verified and thereafter, it was used in a SCC mix for strengthening corroded RC beam to check its flexural behavior compared to a control beam without corrosion.

2. Experimental Program

Ordinary concrete with a 33 MPa compressive strength at 28 days was used to cast the three concrete beams, which were intended to fail in flexural stresses according to the ACI 318-19 [14]. An accelerated corrosion process using Faraday's law was used to get 10% mass loss of tension reinforcement as shown in Fig. 1. After corrosion, the beam was strengthened by applying a U-jacket 30 mm thick layer of the optimized steel fibers reinforced SCC SFRSCC over the sandblasted epoxy coated faces of the RC beam as shown in Fig. 2. The bond between the jacket and the surface of corroded beam was determined using push-out test [15] as shown in Fig. 3. The result of this test indicated that the bond strength was 3.6 MPa. The details of beams including preparation and testing were mentioned in previous research [16]. After the beams were tested, the distractive method was used to calculate the mass losses of corroded longitudinal rebars. In accordance with ASTM G1-3. The bars were chemically cleaned in a solution containing a high concentration of HCl acid to remove rust and related concrete mortar. The following formula was used to calculate mass loss:

$$Mass\ loss = \frac{Mass\ Before\ Corrosion - \ Mass\ After\ Corrosion}{Mass\ Before\ Corrosion} * 100\% \quad (1)$$

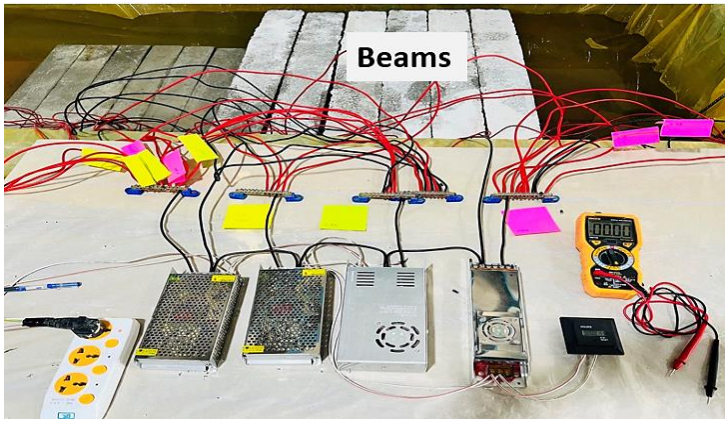

Fig. 1. Corrosion system

Fig. 2. (a) Side view of corroded beam(b)Top view of reference beam (c) Epoxy coating beam before casting (d) Top view of strengthened beam with FRSCC

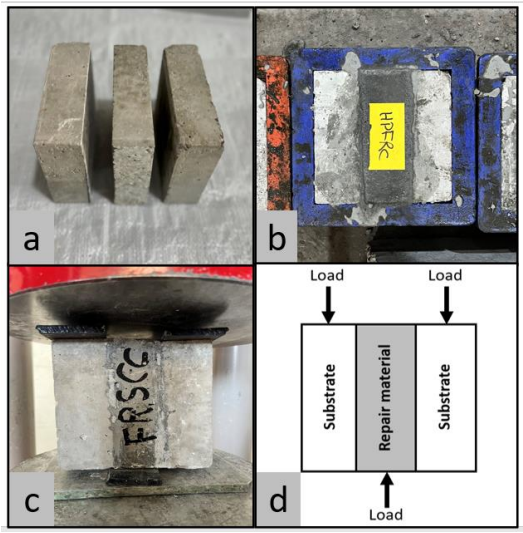

Fig. 3. (a) Cutting of 5 cm-thick concrete blocks (b) casting 5cm-thick of repair concrete (c) test setup (d) test setup diagram

2.1. Materials and Testing Program

2.1.1 Cement C.

Both normal and SCC were produced using Type I ordinary Portland cement. Its beginning and final setting time are 140 and 210 minutes, respectively, and its specific gravity is 3.15. The features of this cement were precisely in accordance with Iraqi requirements and Portland Cement Standard IQS NO. 5, 2019 [17].

2.1.2 Coarse Aggregate C.A.

The maximum size of coarse aggregate used to prepare mixes is 12 mm; it is natural crashed aggregate and it has a specific gravity of 2.65. The test findings of this type of aggregate indicated that it met Iraqi specifications IQS NO. 45, 1984 [18].

2.1.3 Fine Aggregate F.A.

Natural sand was used in this investigation. It is spherical, with a maximum size of 4.75 mm, a specific gravity of 2.62, and a bulk density of 2600 kg/m^3. This type was also identical to the same above Iraqi standard.

2.1.4 Fly Ash FA.

FA with a 2.08 specific gravity and Blaine fineness of 380 m^2/kg was used. It mainly consists of 28% alumina and 47.7% silica. According to ASTM C 618, 2015 [19], this type of mineral filler could be defined as class F.

2.1.5 Silica fume SF.

SF-Type Mega Add MS(D) was used. The silica fume used in this study had a specific gravity of 2.2. According to ASTM C1240, it satisfies the standards for silica fume [20]. Table 1 shows the chemical compositions of C, FA and SF.

Table 1. Chemical compositions of C, FA and SF.

Main oxides %	SiO_2	Al_2O_3	CaO	Fe_2O_3	L.O.I
C	20.06	4.80	62.95	3.35	2.30
FY	47.68	27.73	5.11	18.32	3.71
SF	94.2	0.3	0.27	0.82	3.36

2.1.6 Superplasticizer SP.

Polycarboxylate polymer technology was used having a pH of 4 to 6 and a density of 1.07 kg/liter, that is a high range water reducing super plasticizing admixture. It complies with ASTM C-494 Types G standards [21].

2.1.7 Micro Steel Fibers (MSF).

The steel fibers that were utilized were straight, measuring 15 mm in length and 0.2 mm in diameter. With a minimal tensile strength of 2600 MPa, they were free of corrosion and contaminants.

2.1.8 Epoxy Resin (Sikadure-32 LP)

This resin used as a bonding agent between a concrete jacket for strengthening and corroded RC members. It is applied to the required surface with a thickness of less than 1 mm and has an adhesion strength more than 3 N/mm^2

2.2. Process of Mixing/Casting and Mixing Proportions

The process of preparing fresh SCC mixes involves mixing coarse and fine aggregates in a rotary drum mixer for one minute, followed by pre-mixing cement with CRMs (FA and SF) for two minutes. A small amount of water was added to prevent volatilization. The mixture is then wet mixed for two minutes, then steel fibers were added. SCC mixtures in different fiber ratios are shown in Table 2. After that slump-flow, T500, L-box, and sieve segregation resistance tests were then directly performed. Before casting, each casting mold was thoroughly cleaned and coated with the proper liquid. Following the completion of the concrete mixing procedure, the samples were gradually poured into the prepared molds. On the second day, the samples had been extracted out of the molds, 24 hours later, and put into a tank for water treatment for 28 days before being removed until the test's age [12].

Table 2. Mix proportions in (kg/m^3)

w/c	C	C.A	F. A	W	FA	SF	SP	Steel fiber %
0.4	410	764	970	165	45	45	12.5	*

** Steel fiber %= 0, 0.25, 0.5, 0.75, 1*

2.3. Testing Program

Fresh concrete tests of mixes with different proportions are carried out immediately after mixing. All fresh SCC properties were performed in accordance to EFNARC recommendations (EFNARC, 2005) [22]. According to ASTM C39/C39M [23], the BESMAK-Digital testing compression machine, which has a maximum capacity of 2000 kN, was used. This is for determining the average compressive strength of three-cylinder specimens that measured 100 x 200 mm. In line with ASTM C496/C496M [24] the splitting strength of three 100 x 200 mm cylinders was assessed in the same compressive strength machine at a loading rate of 0.94 kN/s. To find the modulus of rupture, three prisms of 100×100×400 mm were tested using ASTM C78 standard [25].

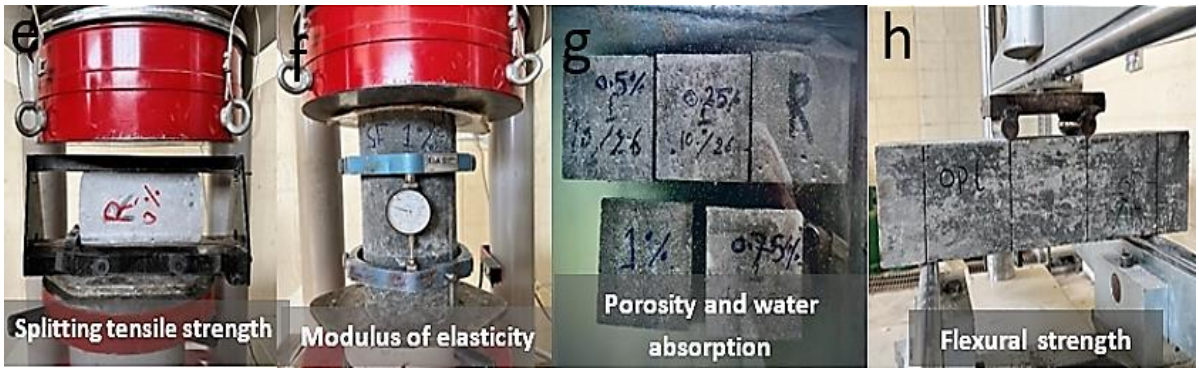

Fig. 4. Fresh (a, b and c) and Mechanical tests (d, e, f, g and h)

The modulus of rupture or flexural strength was measured using a 200 kN hydraulic fracture machine with a 5.3 kN/s rate of loading. Additionally, the elastic modulus was measured in a compressive test machine using an ASTM C469 [26] based cylinder with dimensions of (150×300) mm at a rate of loading of 5.3 kN/s. Due to their major impact on the durability and strength of concrete, experiments on related durability characteristics were also conducted. Following a 28-day cure time, the average of three 100 mm cubic samples were tested for porosity and water absorption tests in accordance with ASTM C642 [27]. The entire performed tests on SCC are shown in Fig. 4.

3. Testing Program

It should be highlighted here that the fresh and mechanical properties of SFRSCC are extensively studied in the literature and the main goal of the current study is not focused in this aspect. The main idea is how to use the results of these tests as multi responses to determine the optimum Vf of steel fibers in SCC. This can give the maximum performance for this type of concrete in an optimized SFRSCC to be used for strengthening purposes. However, quick presentation of the results obtained from tested properties is shown the following section.

3.1. Fresh Properties

Table 3 displays the results of fresh properties tests for each mix of SFRSCC. In general, it is evident that the incorporating of MSF has a negative impact on rheological characteristics but a positive impact on the sieve segregation test. However, all the results still meet with the SCC fresh requirements according to European guidelines EFNARC [22].

Table 3. Fresh properties of SFRSCC mixes.

Mix ID	Vf %	Slump Flow Test (mm)	T500 Test(sec)	L-BOX Test	% Sieve Segregation Test
0M	0	800	2.0	0.95	7.80
0.25M	0.25	800	2.5	0.91	5.00
0.5M	0.5	745	3.0	0.89	4.56
075M	0.75	720	3.5	0.88	3.82
1M	1	710	3.8	0.81	3.46
–	EFNARC limits	650-800	2-5	0.8-1	≤15

The slump flow data shown in Table 3 showed a clear reduction in slump flow values by about 6.8, 10, and 11.25% for the last three mixtures as compared to the reference one (without fibers). Additionally, it was exposed that the T500 values (time to reach a flow of 500 mm) significantly increased by 25, 50, 75, and 90% as compared to reference mix due to the addition of 0.25, 0.5, 0.75, and 1% of steel fibers respectively. This indicates that SCC's viscosity had increased. Increasing the internal friction between MSF and coarse aggregates might explain this phenomenon [22]. In term

of h2/h1 values obtained from L-Box test. The listed results in Table 3 showed that the blocking ratio (h2/h1) for SCC reinforced with MSF reduced by about 4.2, 6.3, 7.3, and 14.7%, respectively as compared to reference mix. This showing clearly how the blocking ratio decreases steadily as MSF increases. The obvious reason for this reduction is that MSF, particularly the large proportion utilized of MSF, prevents the passage of coarse aggregates through steel bars in L-Box test [28, 29].

The segregation indices SI listed in Table 3 displays the effects of adding MSF on SI as a consequence. It can be clearly seen that the incorporating of MSF greatly increases the segregation resistance of SCC mixtures; SI values decreased by about 35.8, 41.5, 51, and 55.6% respectively. This increase is justified by the fact that MSF forms an internal network that might prevent the matrix movement during the sieve segregation test and hence, greatly enhance SCC segregation resistance.

3.2. Mechanical Properties

Fig. 5 (a) illustrates the obtained compressive strength results of SFRSCC mixes. Compared to the reference mix, the values of compressive strength are improved by 13.6, 18.9, 20.9, and 22.9% respectively as the fiber's contents were increased. These findings are in line with the previous research [30]. Such improvement is justified by the function served by MSF in restricting the development of cracks as well as by the strong connection between MSF and the SCC matrix [31]. Moreover, it is shown that the presence of MSF modified the loading failure mode. It is noted that the plain SCC show a complete collapse in its failure mode. However, the specimens reinforced by MSF display a more ductile failure mode with the increase of MSF content. The restriction of MSF of concrete pieces, which helps to prevent rapid failure, is responsible for this change as shown in Fig. 5 (b). For example, reference mix (0M) exhibited explosive failure mode. In contrast, 1M mix which contained the highest fiber volume fraction showed completely bridging failure mode.

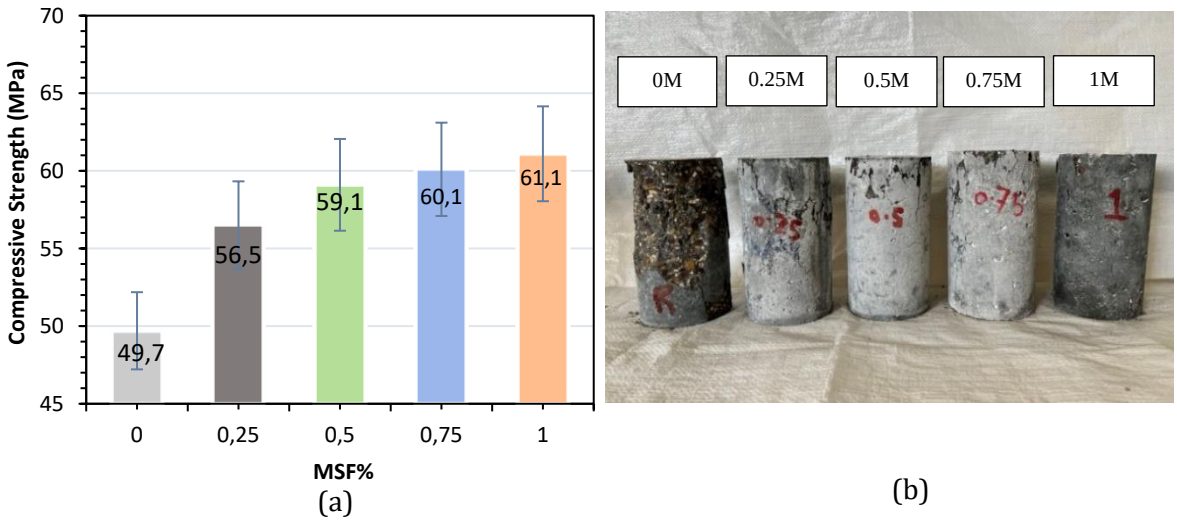

Fig. 5. Compressive strength results (a) values for various amounts of steel fibers at 28 days (b) failure mode after compressive strength test

In Fig. 6 (a) the results of the flexural and splitting strengths are displayed. It has been shown that SCC mixtures were greatly enhanced in term of their flexural strength values. The flexural strength values increased by 47.05, 51.4, 55.8, and 77.9% due to the incorporation of 0.25, 0.5, 0.75, and 1% respectively. The splitting tensile strength also significantly enhanced when the MSF volume fraction increased. These increments were: 51.2, 56.4, 64.1, and 112.8% respectively as compared to reference SCC. As illustrated in Fig. 6 (b), MSF resists the rapid failure of plain SCC specimens by bridging fractures sides under tensile stress. According to Fig. 6, the four-volume fractions of MSF resulted in a rise in the modulus of elasticity of 5.7, 8.7, 13.6, and 18.3%, respectively, in comparison to the reference mix as shown in Fig.7. The observed increases in compressive and tensile strengths may be related to this trend. For instance, 0M mix showed very brittle failure mode in flexural and splitting tensile strengths, while 1M mix exhibited ductile failure mode in these two tests.

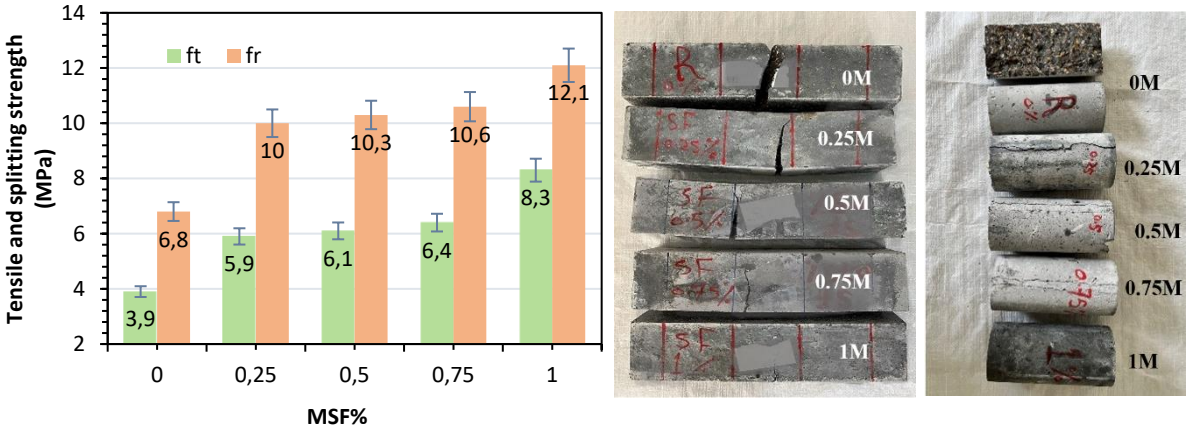

(a) (b)

Fig. 6. Flexural and splitting strength results (a) various amounts of steel fibers values at 28 days (b) failure mode after flexural and splitting strength test

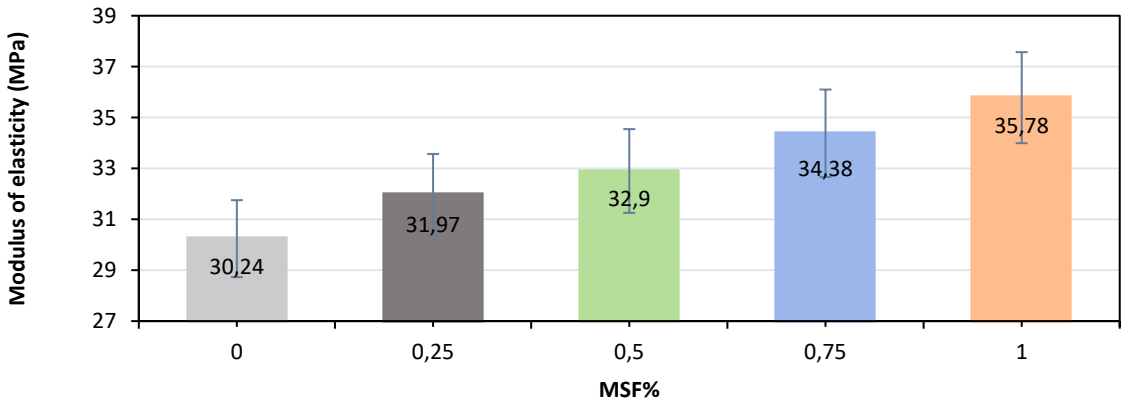

Fig. 7. Modulus of elasticity values for various amounts of steel fibers at 28 days

3.3. Related Durability Properties

According to the study, the values of porosity and water absorption of concrete rise with the amount of steel fiber contained as shown in Fig. 8. This could be due to the creation of voids within the concrete sample, which could be caused by the interruption of water flow beneath the fibers. The number of fibers in the SCC mix has negative impact on both water absorption and porosity results as claimed by Suleman et al. [32].

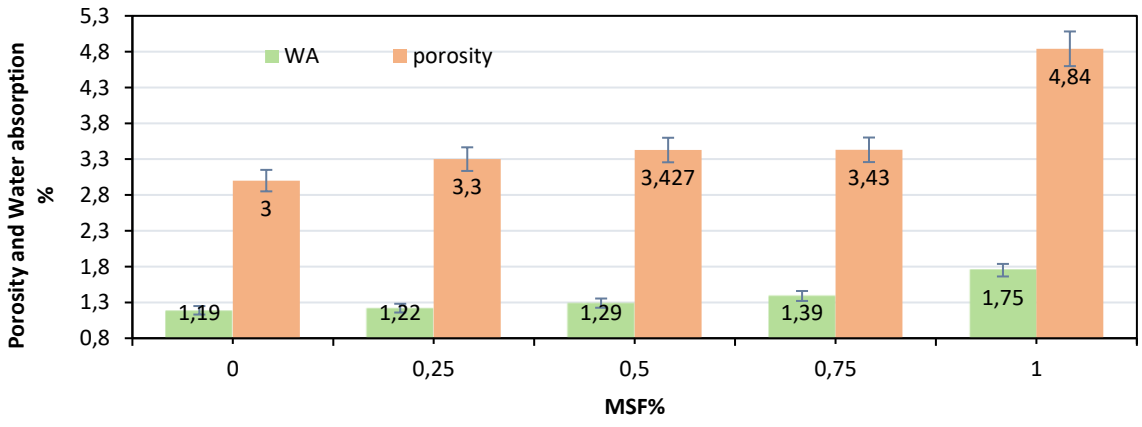

Fig. 8. Relationships between porosity, water absorption, and MSF for SCC mixtures

3.4. Optimization of the Properties of SCC Mixes

Table 4 summarizes the results from the previous section for multi-objective optimization. No fiber content can provide the best properties of fresh and mechanical simultaneously. Therefore, an optimal fiber content between tested ratios is needed for an excellent SCC mix.

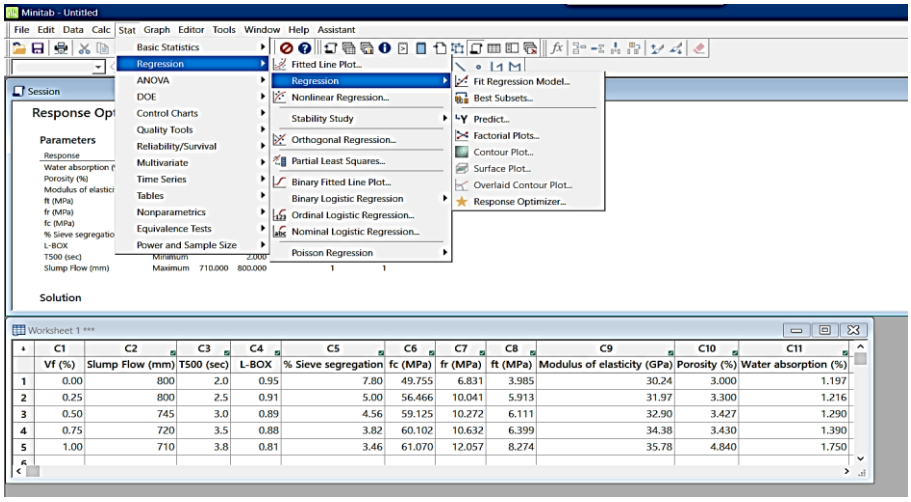

	C1	C2	C3	C4	C5	C6	C7	C8	C9	C10	C11
	Vf (%)	Slump Flow (mm)	T500 (sec)	L-BOX	% Sieve segregation	fc (MPa)	fr (MPa)	ft (MPa)	Modulus of elasticity (GPa)	Porosity (%)	Water absorption (%)
1	0.00	800	2.0	0.95	7.80	49.755	6.831	3.985	30.24	3.000	1.197
2	0.25	800	2.5	0.91	5.00	56.466	10.041	5.913	31.97	3.300	1.216
3	0.50	745	3.0	0.89	4.56	59.125	10.272	6.111	32.90	3.427	1.290
4	0.75	720	3.5	0.88	3.82	60.102	10.632	6.399	34.38	3.430	1.390
5	1.00	710	3.8	0.81	3.46	61.070	12.057	8.274	35.78	4.840	1.750

(a)

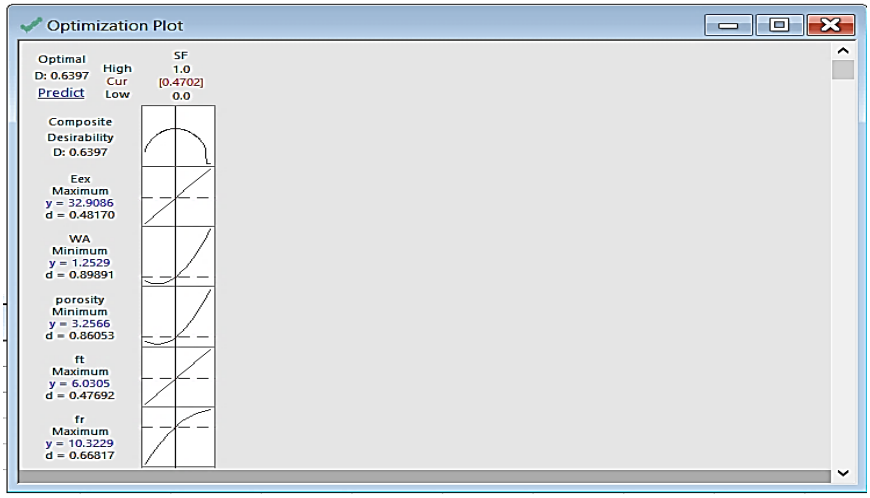

(b)

Response Optimization: Water absorption (%), Porosity ... Flow (mm)

Parameters

Response	Goal	Lower	Target	Upper	Weight	Importance
Water absorption (%)	Minimum		1.197	1.75	1	1
Porosity (%)	Minimum		3.000	4.84	1	1
Modulus of elasticity (GPa)	Maximum	30.240	35.780		1	1
ft (MPa)	Maximum	3.985	8.274		1	1
fr (MPa)	Maximum	6.831	12.057		1	1
fc (MPa)	Maximum	49.755	61.070		1	1
% Sieve segregation	Minimum		3.460	7.80	1	1
L-BOX	Maximum	0.810	0.950		1	1
T500 (sec)	Minimum		2.000	3.80	1	1
Slump Flow (mm)	Maximum	710.000	800.000		1	1

(c)

Fig. 9. Optimization using Minitab: a) optimization steps b) optimization plot c) goal and targets of optimization

This mixture should have the highest flow, compressive, flexural, tensile, and elastic modulus, with the least amount of porosity and water absorption. The results were analyzed using the Minitab 2018 statistical program Fig.9 to find the optimum ratio, which was determined to be 0.47%, providing the most desirable characteristics.

Table 4. Summary of responses used for optimization

Mix ID	Slump Flow (mm)	T500 (sec)	L-BOX	% Sieve segregation	fc (MPa)	fr (MPa)	ft (MPa)	Modulus of elasticity (GPa)	Porosity (%)	Water absorption (%)
0M	800	2.0	0.95	7.80	49.755	6.831	3.985	30.24	3	1.197
0.25M	800	2.5	0.91	5.00	56.466	10.041	5.913	31.97	3.3	1.216
0.5M	745	3.0	0.89	4.56	59.125	10.272	6.111	32.9	3.427	1.29
0.75M	720	3.5	0.88	3.82	60.102	10.632	6.399	34.38	3.43	1.39
1M	710	3.8	0.81	3.46	61.07	12.057	8.274	35.78	4.84	1.75

3.5. Validation of Theoretical Optimization

The optimal mix was produced and tested in order to validate the prior theoretical multi-objective optimization in order to check the accuracy of this optimization. In a controlled environment, the optimal mixture was produced using a similar ingredient and amounts of the materials that were predicted theoretically. Eq (2) is used to calculate the absolute relative deviation ARD% as a predictability indicator [33]. Theoretical and experimental obtained results as well as ARD% are listed in Table 5.

$$ARD\% = 1 - \frac{[Experimental - Model\ or\ Model - Experimental]}{Experimental} * 100\% \quad (2)$$

Table 5. Results and experimental validation of optimum mix

Type	Slump Flow (mm)	T50 0 (sec)	L-BOX	% Sieve Segregation	Fc (MPa)	Fr (MPa)	Ft (MPa)	Ec (GPa)	Porosit y %	Water Absorptio n %
Exp.	750	2.0	0.9	4.2	57.23	10.3	7.48	32.7	3.36	1.27
Theoretical	756.68	2.96	0.898	4.39	58.85	10.32	6.03	32.9	3.25	1.25
ARD %	99.10	52	99.77	95.47	97.16	99.80	80.61	99.38	96.72	98.42

The theoretical predicted results were very closed to the experimental ones indicating a very high accuracy of the proposed models. The only exception is the ARD of T500 which was only 52%. The reason might be related to the short time of this test (below 5 sec) and small change of these seconds will affect the result considerably. These results are on line with number of previous studies as in Mahmoud et al. and Fayad et al [34, 35].

3.6. Flexural Test Results

The experimental test results are summarized in Table 6 and include the following: the largest crack measured for the greater fracture on the face of the beam at failure, load at first flexural crack (Pcr), ultimate load (Pu), deflection at first crack (Δcr), and deflection at ultimate load (Δu). Furthermore, the flexural stiffness (k) was determined by calculating the slope (ΔF/Δδ) of the linear component of the load-deflection curves between 10% and 50% of the maximum load [36]. It is clear from the Table 6 that the bearing capacity of corroded beam was less than uncorroded beam by about 9.42% as for deflection and stiffness. This reduction is a result of a decrease of the cross-sectional area during the accelerating corrosion process. The corroded RC beam strengthens by optimized fiber reinforced self-compacting concrete jacket increased the efficiency of bearing capacity by 19.84%. After the reinforcing steel is yielded, the strengthening layer begins to bear until failure, and this is consistent with the results obtained by Huang et al. [37]. The observed

increase in deflection and crack width in the strengthened beam aligns with the expected structural response following the application of a 30-mm SFRSCC jacket.

Table 6. Flexural test results

Beam ID	(Pu) (kN)	(Pcr) (kN)	Change percent in Pu with respect to BR	(Δu) (mm)	(Δcr) (mm)	Max. crack width at failure (mm)	Stiffness (kN/mm)
Ref. RC Beam (BR)	100	25	-	17.65	0.56	3.5	35.66
Ref. Corroded RC Beam	90.58	25	-9.42	16.17	0.57	6.7	32.35
Strengthen Corroded RC Beam	108.56	40	+8.56	19.7	0.64	20	44.31

The added layer alters the stiffness distribution along the beam depth, causing a downward shift of the Neutral Axis (NA) and consequently increasing the tensile strain demand in the extreme tension fiber. Under comparable loading, this results in larger tensile strains at the bottom surface, naturally leading to wider flexural cracks. Importantly, the absence of delamination indicates that the shear stresses were effectively transferred across the old–new concrete interface. The roughened substrate surface provided mechanical interlock, while the SFRSCC jacket ensured high bond strength and fiber-induced confinement, preventing localized interface cracking. As a result, the jacket–substrate interface behaved monolithically, ruling out debonding failure. Instead, the shear forces were transmitted into the strengthened section, producing two opposite diagonal cracks at approximately 45° within the middle third of the beam. The lack of vertical mid-span cracks excludes flexural failure, and the observed diagonal tension cracks propagating toward the compression zone confirm that the beam reached its shear capacity, consistent with internal shear failure in strengthened RC members as shown in Fig. 9. Based on this result, it can be concluded that the used method for strengthening was effective. It should be highlighted that the corresponding service crack (the crack at approximately 70% of ultimate load [38]) is equal to only 0.4 mm. Due time limitation, the long-term behavior of the strengthen system was not considered and it needs further future research work.

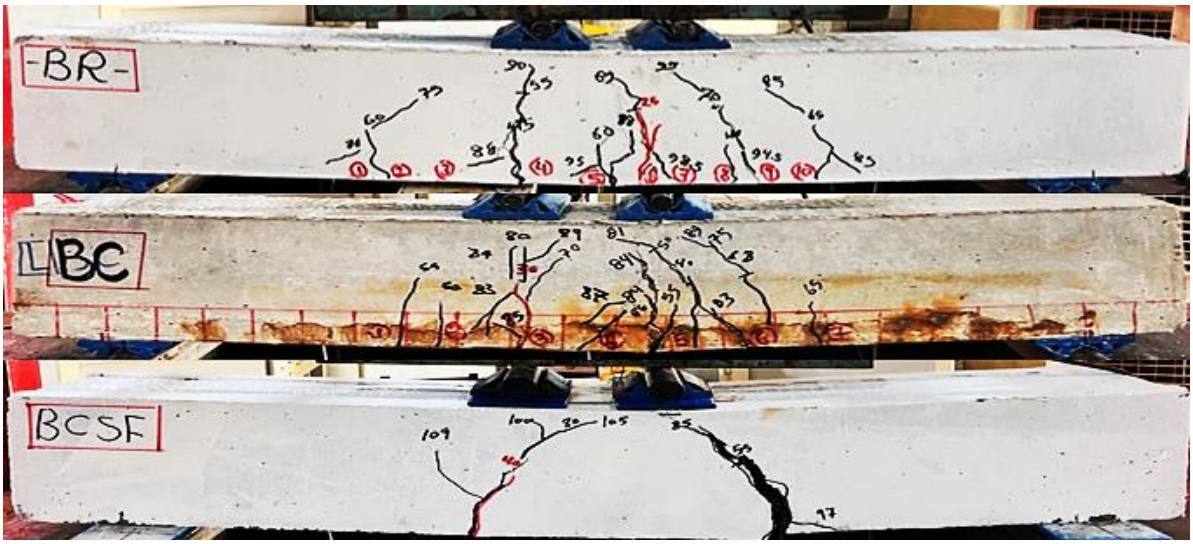

Fig. 9. Failure modes

4. Conclusion

The most significant findings from this investigation can be summed up as follows:

- Increasing fiber content has a negative impact on SFRSCC fresh characteristics, with the exception of the sieve segregation test.
- Compressive strength and elastic modulus of SFRSCC mixes slightly increased as steel fiber content increased; however, significant improvement be recorded in tensile test results at the same volume fractions of steel fibers.
- The obtained results suggested that increase of micro steel fiber content raised the flexural strength significantly and changed the failure mode to be more ductile.
- The porosity and water absorption values considerably increased with the proportion of steel fiber content in particular, at 1% Vf. Porosity and absorption were greater by 61.3% and 46.2%, respectively for this mix as compared to control one.
- Based on the multi objective optimization results, the optimum theoretical steel fiber content for SCC was 0.47%, which provided good mechanical strength and durability features. These data were produced using statistical software and optimization (Minitab 2018).
- Based on the tests for the theoretical optimized mixture, the theoretical value of Vf (0.47%) was verified experimentally to give the same expected performance
- The experimental results of mass loss were exactly similar to those of theoretical calculation using Faraday's law with 10%.
- The bearing capacity of corroded beam was less than uncorroded beam by about 9.42%.
- The bearing capacity of corroded RC beam strengthens by fiber reinforced self-compacting concrete jacket increased by 19.84% compared to corroded one.
- The first crack appeared in the strengthened beam only after the load reached 40 MPa, unlike the non-corroded and corroded reference beams where the first crack appeared at a load of 25 MPa.
- The strengthened beam exhibited a shear-controlled failure mode.
- Corroded reinforced concrete beams can probably be strengthened using U-jacket of optimized FRSCC mix which can be considered as an efficient strengthening technique.
- Investigating the efficiency of using fiber reinforced high strength lightweight concrete for strengthening corroded beams need to be studied.

References

[1] EFNARC. Guidelines for self-compacting concrete. English ed. European Federation for Specialist Construction Chemicals & Concrete Systems; 2005.
[2] Iqbal S, Ali A, Holschemacher K, Bier TA. Effect of change in micro steel fiber content on properties of High strength Steel fiber reinforced Lightweight Self-Compacting Concrete (HSLSCC). Procedia Eng. 2015;122:88-94. https://doi.org/10.1016/j.proeng.2015.10.011
[3] Puskas A, Moga L. Sustainability of reinforced concrete frame structures-A case study. Int J Sustain Dev Plan. 2015;10(2):165-176. https://doi.org/10.2495/SDP-V10-N2-165-176
[4] Saba AM, Khan Az, Niazi MSK, Farooq F, Javed MF, Aslam F, et al. Strength and flexural behavior of steel fiber and silica fume incorporated self-compacting concrete. J Mater Res Technol. 2021;12:1380-1390. https://doi.org/10.1016/j.jmrt.2021.03.066
[5] Zhao Y, Bi J, Guan J, Mao R, Huo L, Zhang S, et al. Synergetic effect of ground granulated blast-furnace slag and hooked-end steel fibers on various properties of steel fiber reinforced self-compacting concrete. Struct Concr. 2022;23(1):268-284. https://doi.org/10.1002/suco.202000722
[6] Farooq F, Jin X, Javed MF, Akbar A, Shah MI, Aslam F, et al. A comparative study for the prediction of the compressive strength of self-compacting concrete modified with fly ash. Materials. 2021;14(17):4934. https://doi.org/10.3390/ma14174934
[7] Alaloul WS, Musarat MA, Liew MS, Law K, Sharafuddin MA, Alawag AM, et al. Mechanical properties of silica fume modified high-volume fly ash rubberized self-compacting concrete. Sustainability. 2021;13(10):5571. https://doi.org/10.3390/su13105571
[8] Frazão C, Camões A, Barros J, Gonçalves D. Durability of steel fiber reinforced self-compacting concrete. Constr Build Mater. 2015;80:155-166. https://doi.org/10.1016/j.conbuildmat.2015.01.061

[9] El-Dieb A, Taha MR. Flow characteristics and acceptance criteria of fiber-reinforced self-compacted concrete (FR-SCC). Constr Build Mater. 2012;27(1):585-596. https://doi.org/10.1016/j.conbuildmat.2011.07.004
[10] Abid SR, Abdul-Hussein ML, Ali SH, Kazem AF, Al-Gasham TS. Impact performance of steel fiber-reinforced self-compacting concrete against repeated drop weight impact. Crystals. 2021;11(2):91. https://doi.org/10.3390/cryst11020091
[11] Koulouris K, Apostolopoulos C. An experimental study on effects of corrosion and stirrups spacing on bond behavior of reinforced concrete. Metals. 2020;10(10):1327. https://doi.org/10.3390/met10101327
[12] Fayaad TS. Strengthening of Corroded Reinforced Concrete Beams by SCC Using Different Strengthening Configurations [Thesis]. Anbar: University of Anbar; 2022.
[13] Abdulhameed HA, Nassif H, Khayat KH. Use of fiber-reinforced self-consolidating concrete to enhance serviceability performance of damaged beams. Transp Res Rec. 2018;2672(27):45-55. https://doi.org/10.1177/0361198118787983
[14] ACI Committee 318. Building Code Requirements for Structural Concrete (ACI 318-19) and Commentary. Farmington Hills, MI: American Concrete Institute; 2019.
[15] Ghodousian O, Shetabivash H, Alipour R, Ozbakkaloglu T. Interfacial bond strength of coloured SCC repair layers: an experimental and optimisation study. J Struct Integr Maint. 2023:1-10.
[16] Mahmoud NA, Mansoor YA, Mohammed MK. Structural behaviors of different corroded RC members strengthened by different types of concrete jackets. Salud, Ciencia y Tecnología-Serie de Conferencias. 2024 (3), 831. https://doi.org/10.56294/sctconf2024831
[17] Iraqi Quality Standards (IQS). Iraqi specification for Portland Cement requirements. IQS 5; 2019.
[18] Iraqi Quality Standards (IQS). Aggregate from Natural Sources for Concrete and Construction. IQS 45. Baghdad: Central Agency for Standardization and Quality Control; 1984.
[19] ASTM International. ASTM C618-15: Standard Specification for Coal Fly Ash and Raw or Calcined Natural Pozzolan for Use in Concrete. West Conshohocken, PA; 2015.
[20] ASTM International. ASTM C1240-05: Standard specification for silica fume used in cementitious mixtures. West Conshohocken, PA; 2005.
[21] ASTM International. ASTM C494/C494M-17: Standard Specification for Chemical Admixtures for Concrete. West Conshohocken, PA; 2017.
[22] BIBM, et al. The European guidelines for self-compacting concrete. 2005;22:563.
[23] ASTM International. ASTM C39/C39M-20: Standard Test Method for Compressive Strength of cylindrical Concrete Specimens. West Conshohocken, PA; 2020.
[24] ASTM International. ASTM C496/C496M-11: Standard Test Method for Splitting Tensile Strength of Cylindrical Concrete Specimens. West Conshohocken, PA; 2011.
[25] ASTM International. ASTM C78/C78M-18: Standard Test Method for Flexural Strength of Concrete Using Simple Beam with Third-Point Loading. West Conshohocken, PA; 2018.
[26] ASTM International. ASTM C469/C469M-14: Standard Test method for static modulus of elasticity and poisson's ratio of concrete in compression. West Conshohocken, PA; 2014.
[27] Bu Y, Spragg R, Weiss W. Comparison of the pore volume in concrete as determined using ASTM C642 and vacuum saturation. Adv Civil Eng Mater. 2014;3(1):308-315. https://doi.org/10.1520/ACEM20130090
[28] Grünewald S, Walraven JC. Parameter-study on the influence of steel fibers and coarse aggregate content on the fresh properties of self-compacting concrete. Cem Concr Res. 2001;31(12):1793-1798. https://doi.org/10.1016/S0008-8846(01)00555-5
[29] Irki I, Debieb A, Settari C, Khatib JM, Kenai S. Effect of the length and the volume fraction of wavy steel fibers on the behavior of self-compacting concrete. J Adhes Sci Technol. 2017;31(7):735-748. https://doi.org/10.1080/01694243.2016.1231394
[30] Mastali M, Dalvand A. Use of silica fume and recycled steel fibers in self-compacting concrete (SCC). Constr Build Mater. 2016;125:196-209. https://doi.org/10.1016/j.conbuildmat.2016.08.046
[31] Bazgir A. The behaviour of steel fibre reinforced concrete material and its effect on impact resistance of slabs [MPhil Thesis]. London: City University London; 2016.
[32] Suleman D, Mohammed MK, Mansoor YA. Optimization of Different Properties of Ultra-High Performance Concrete Mixes for Strengthening Purposes. Iraqi J Civil Eng. 2022;15(2):72-85. https://doi.org/10.37650/ijce.2021.172875
[33] Hussien AS, Mohammed MK. Optimum characteristics of plastic fibres for sustainable self-compacting concrete SCC. Eur J Environ Civil Eng. 2022:1-18. https://doi.org/10.1080/19648189.2022.2119605
[34] Mohammed MK, Al-Hadithi AI, Mohammed MH. Production and optimization of eco-efficient self compacting concrete SCC with limestone and PET. Constr Build Mater. 2019;197:734-746. https://doi.org/10.1016/j.conbuildmat.2018.11.189

[35] Fayaad TS, Mohammed MK, Mansoor YA. Optimization of different types of self-compacting concrete mixes for strengthening purposes. AIP Conf Proc. 2024. https://doi.org/10.1063/5.0190534
[36] Najim KB. Determination and enhancement of mechanical and thermo-physical behaviour of crumb rubber-modified structural concrete [Thesis]. University of Nottingham; 2012.
[37] Huang Y, Li J, Hong S, Wu X, Huang J. Reinforced concrete beams retrofitted with UHPC or CFRP. Case Stud Constr Mater. 2022;17:e01507. https://doi.org/10.1016/j.cscm.2022.e01507
[38] Tayeh BA, Maraq MAA, Ziara MM. Flexural performance of reinforced concrete beams strengthened with self-compacting concrete jacketing and steel welded wire mesh. Structures. 2020;27:1477-1488. https://doi.org/10.1016/j.istruc.2020.10.035